PROCEEDINGS OF SCIENCE

Time-of-flight detector for the identification of low-momentum secondary cosmic rays in the ACROMASS experiment

Diletta Borselli,[a,b,*] **Adriani Oscar,**[a,b] **Lorenzo Bonechi,**[a,b] **Massimo Bongi,**[a] **Carlo Cialdai,**[b] **Roberto Ciaranfi,**[b] **Raffaello D'Alessandro,**[a,b] **Sebastiano Detti,**[b] **Catalin Frosin,**[b] **Paolo Papini,**[b] **Sergio Bruno Ricciarini**[c] **and Monica Scaringella**[b]

[a] *Department of Physics and Astronomy, University of Florence, Via Sansone 1, Sesto Fiorentino, Florence*

[b] *National Institute of Nuclear Physics (INFN), Florence Division Via Bruno Rossi 1, Sesto Fiorentino, Florence*

[c] *Consiglio Nazionale delle Ricerche (CNR), Florence Via Madonna del Piano 10, Sesto Fiorentino, Florence*

E-mail: diletta.borselli@fi.infn.it, diletta.borselli@unifi.it

The knowledge of the atmospheric muon flux in cosmic rays at ground level is of considerable interest in various particle physics and applied physics experiments, in particular to calibrate Monte Carlo models used in atmospheric shower simulations and for precision studies of neutrino oscillations. In the literature there is no systematic study of the muon component at ground level at different measurement points on the Earth's surface (latitude, longitude and altitude). The ACROMASS (Atmospheric Cosmic Ray Observatory using a Magnetic Altazimuth Silicon Spectrometer) experiment of the National Institute for Nuclear Physics (INFN Italy) aims to study the main components of secondary cosmic rays at ground level with particular attention to low-energy components. ACROMASS includes some sub-detectors such as a magnetic spectrometer, a TOF (time-of-flight) and an electromagnetic calorimeter that have the task of performing Particle-IDentification (PID). The TOF subdetector, designed to discriminate between muons and protons at low momentum ($p < 1\mathrm{GeV}/c$), will be presented. The detector, consisting of fast segmented plastic scintillators and silicon photomultipliers as light sensors, is coupled to a high temporal resolution readout electronics, the SAMPIC module designed by a collaboration including CEA/IRFU/SEDI Saclay (France) and CNRS/LAL/SERDI Orsay (France). The detector and the first tests carried out on its operation in terms of temporal performance will be presented.

39th International Cosmic Ray Conference (ICRC2025)
15–24 July 2025
Geneva, Switzerland

*Speaker

PoS(ICRC2025)200

1. Introduction

A detailed understanding of the flux of secondary cosmic rays at ground level is of significant interest in both fundamental and applied physics. In particular, accurate knowledge of the atmospheric muon flux at ground level is crucial for precision measurements of atmospheric neutrino oscillations [1]. It is also essential for the normalization of muography data [2]. Muography is a relatively recent imaging technique that uses muon transmission to infer the density of large-scale structures, such as volcanoes, mines, industrial and civil infrastructure, and archaeological sites [3–9].

When a primary cosmic ray (mostly protons) enters the upper atmosphere, it interacts with atmospheric nuclei, producing a cascade of secondary particles [10, 11]. This shower propagates through the atmosphere, generating numerous particles, some of which are absorbed while less others reach the Earth's surface. The majority of the charged particles arriving at ground level are muons, electrons, positrons, and protons [11].

Studies reported in [1] have shown that experimental uncertainties in atmospheric muon neutrino oscillation measurements decrease with improved precision in the determination of the ground-level muon flux. The correlation between the muon and neutrino fluxes becomes particularly significant at energies below 1 GeV. Atmospheric showers are modeled using Monte Carlo algorithms, which are calibrated through measurements taken at a few different locations worldwide and from different detectors, as well as from dedicated measurements at particle accelerators. Direct measurement of secondary cosmic ray components at ground level as a function of geographical location is essential for the calibration of these simulation codes.

Currently, no experiments worldwide are specifically designed to perform systematic measurements of the energy and angular spectrum of ground level muons across different geographical sites. The ACROMASS (Atmospheric Cosmic Ray Observatory using a Magnetic Altazimuth Silicon Spectrometer) experiment aims to assemble a portable detector capable of discriminating the muon component from other charged components (such as electrons and protons) and of conducting measurements at various locations around the globe (sites coinciding with neutrino experiments are of particular interest for calibration with data).

As described in Section 2, the detector, currently under assembly, consists of several sub-detectors that enable particle identification. In particular, Section 3 will focus on the TOF (time-of-flight) sub-detector, which is designed for low-energy muon-proton discrimination.

2. The ACROMASS experiment

The ACROMASS experiment (Atmospheric Cosmic Ray Observatory using a Magnetic Altazimuth Silicon Spectrometer) represents an evolution of the ADAMO experiment [12], developed in the early 2000s at the University of Florence and the National Institute of Nuclear Physics (INFN), Florence division. The ADAMO experiment, based on a magnetic spectrometer, enabled the study of the energy spectrum of cosmic rays at ground level as a function of the zenith angle α, but did not allow for particle identification (see figure 1 left panel for results).

ADAMO was itself a prototype of the magnetic spectrometer of the PAMELA satellite experiment [13], which was launched into orbit in 2006. ADAMO consisted of a silicon microstrip

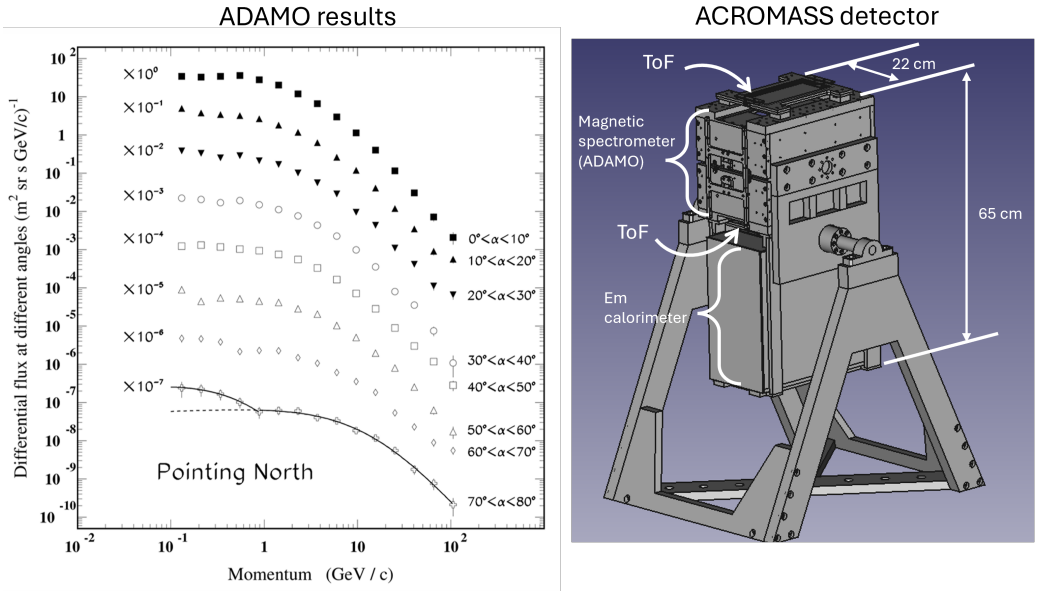

Figure 1: On the left, results obtained in 2004 in Sesto Fiorentino near Florence with the ADAMO experiment, which now constitutes the core of the ACROMASS apparatus. The momentum spectrum of cosmic rays detected at ground level is shown as a function of the zenith angle α. On the right, the schematic layout of the ACROMASS experiment, illustrating the configuration of its three sub-detectors: the time of-flight (TOF) system, the magnetic spectrometer, and the electromagnetic calorimeter

tracker composed of five detection planes, with spatial resolution on both x and y coordinates of approximately ($\sigma_x \sim 3\,\mu$m, $\sigma_y \sim 13\,\mu$m), and a permanent magnet providing a magnetic field of about 0.4 T. The system was capable of measuring particle rigidity up to approximately 250 GV/c.

The ACROMASS experiment is designed with multiple sub-detectors, as illustrated in figure 1 (right), to enable particle identification (PID). The detector is currently under assembly and is expected to be ready for high-altitude measurements by the end of 2026. At the core of the setup lies the magnetic spectrometer from the ADAMO experiment, to which a Time-of-Flight (TOF) system and an electromagnetic calorimeter have been added. All components are mounted on a mechanical structure that allows the entire detector to be oriented like a telescope. The TOF system consists of two fast plastic scintillators coupled to Silicon Photomultipliers (SiPMs) characterized by very short rise times. The TOF planes are positioned above and below the magnet and enable muon–proton discrimination at low energies. Further technical details of the TOF system are provided in section 3. The electromagnetic calorimeter, located beneath the other detection systems, enables high-energy particle identification by analyzing the development of the shower inside. It is specifically optimized for distinguishing muons from electrons and protons. The total expected weight of the apparatus is approximately 100 kg, with overall dimensions (excluding the rotating platform) of about $(20 \times 30 \times 60)$ cm.

Measurements performed with the ADAMO experiment show (figure 1, left) an increase in the detected particle flux below 1 GeV/c, suggesting a possible contamination from the electronic component. These data were collected in Sesto Fiorentino, near Florence (Italy). The ACROMASS experiment is expected to improve upon these results by enabling discrimination between the

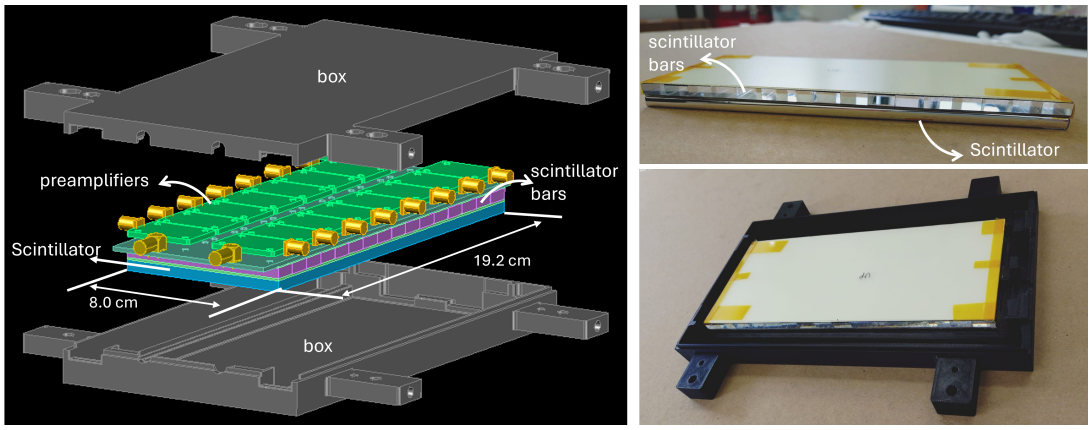

Figure 2: On the left is a CAD drawing of one of the two TOF detectors. The preamplifiers are located directly above the scintillators. On the right photographs of the detector during assembly are shown.

various components of the cosmic ray flux. This energy range is of interest for studies on neutrino oscillations [1]. In particular, it will allow for a separation of the muonic, electronic, and hadronic contributions, providing a more accurate characterization of the spectrum. Currently, ADAMO data are used in simulation frameworks such as EcoMug [14] (presenting some issues as explained in [2]), serving as input for atmospheric muon generation and detector response modeling.

3. The time-of-flight detector

The time-of-flight (TOF) detector of the ACROMASS experiment is currently under assembly and has been designed to enable discrimination between muons and protons below 1 GeV/c up to 0.1 GeV/c. It consists of two scintillation detectors positioned above and below the magnetic spectrometer, as shown in figure 1, right. Each detector is composed of two scintillator planes with total dimensions of $(5 \times 192 \times 80)$ mm arranged one above the other, as illustrated in figure 2. Both planes are housed within the same enclosure together with the readout electronics.

The upper scintillator plane is segmented; it consists of 16 plastic scintillator bars with dimensions of (5×12×80), mm arranged side-by-side to form a complete plane. This segmentation enables the reconstruction of the particle impact position along one direction, which can be compared and corrected with the track reconstructed by the silicon tracker of the magnetic spectrometer (although with lower precision). Furthermore, segmentation improves the detector's timing response by accelerating the signal collection, thus optimizing the time-of-flight measurement. Aluminized Mylar sheets have been placed between the contact faces of the bars to provide optical isolation. The presence of the non-segmented lower scintillator plane allows for the evaluation of the efficiency of the segmented bar plane used for the time-of-flight measurements.

The organic scintillators used are the EJ-232-Q-(0.5% Benzophenone) from the company ELJEN Tecnhology [15] whose main characteristics are found in the table 1. They are fast scintillators with rise times of 1.1 ns.

Each small face of every scintillator bar is coupled to two SiPMs, for a total of four SiPMs per bar. The four signals are combined in parallel to produce a single output signal per bar. This configuration makes the signal development within the bar independent of the particle impact

EJ 232 Q (0.5%Benzophenone)	
Light Output (% Anthracene)	19
Scintillation Efficiency (photons/1 MeV e-)	2,900
Wavelength of Maximum Emission (nm)	370
Rise Time (ps)	110
Decay Time (ps)	700
Refractive Index	1.58

Table 1: EJ-232-Q-0.5% Benzophenone ELJEN Tecnhology scintillator main characteristics.

position, optimizing the light collection time and providing an overall higher output signal compared to a single SiPM. The SiPMs used are the Onsemi J-Series 30035 model, with active areas of $(4 \times 4)\,\mathrm{mm}^2$ and rise times between 90 and 110 ps, depending on the overvoltage, which ranges from +2.5 V to +6 V, respectively. Further specifications can be found in [16]. The lower scintillator plane is coupled, via optical cement, to 4 SiPMs per face, totaling 8 SiPMs on two opposite faces. In this case as well, the electronics sums the signals from all eight SiPMs. All signals are followed by an amplification stage located directly on the front-end electronics housed within the same box as the scintillators (figure 2 on the left). The mechanical housing was fabricated using 3D printing and is made of plastic material, thus reducing the overall weight of the apparatus.

The amplified signals from each scintillator are sent to a 32-channel digitizer. The chosen digitizer is the SAMPIC module [17], designed by a collaboration including CEA/IRFU/SEDI, Saclay and CNRS/LAL/SERDI, Orsay. This digitizer, with a sampling capability of up to 6.4 Gs/s, enables time measurements with very high accuracy, reaching resolutions on the order of picoseconds. The module has already been employed in experiments requiring high temporal resolution at particle accelerators such as ATLAS, CMS, and TOTEM, as well as in medical imaging applications. The module features a graphical user interface compatible with Windows operating systems, allowing for configuration and data saving on a PC. It was used for the initial tests on the scintillator bars and, as described in section 4, for a preliminary estimate of the timing resolution of the scintillator–SiPM–electronics system, which is essential to determine the energy range in which the TOF detector can perform particle discrimination.

Currently, the apparatus is in the assembly and testing phase, with operational readiness expected within the next few months.

4. Preliminary temporal resolution measurements and results

A preliminary study was conducted to evaluate the time resolution of the experimental setup composed of scintillator bars, SiPMs, and the SAMPIC digitizer. The test was performed using only two scintillator bars, placed one on top of the other in direct contact [18]. For this test, each bar was paired with two SiPMs per bar on only one face (see figure 3, left). The SiPMs on each bar were connected in parallel in the front-end electronics to produce a single output signal per bar. This signal was then amplified and sent to the SAMPIC module. The distribution of the time difference between the arrival of the signals from the two bars provides an estimate of the timing resolution of the system σ_{tof}. This estimate includes the contribution to the time difference ($\sigma_{\text{point}} \sim 88.5\,\text{ps}$

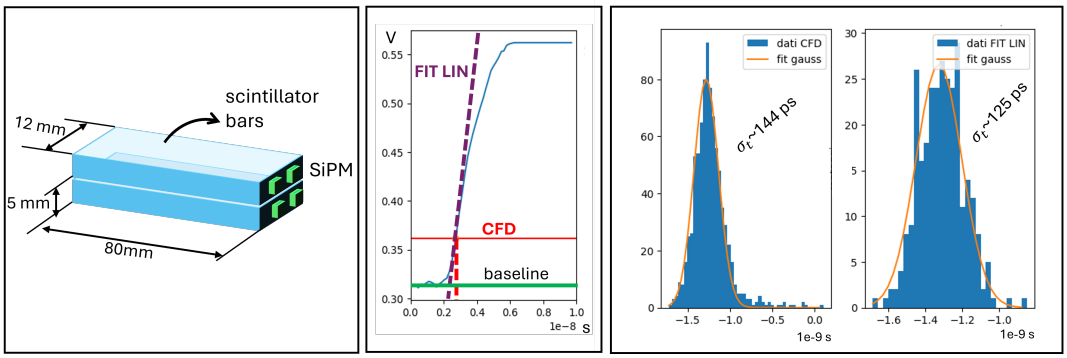

Figure 3: On the left is shown the scheme of the experimental setup for the estimation of the temporal resolution of the two-bar system. In the center the two algorithms chosen for determining the timestamp are shown: the constant fraction discriminator (CFD) method and the linear fit method (FIT LIN). On the right is shown the distribution of the temporal difference of the signals from the upper and lower bar corresponding to the CFD method and the linear fit method.

estimated in [18]) arising from the particle's impact point on the scintillator bar and the inclination of its trajectory. In the final design, this additional contribution will be evaluated using the micrometric precision of the silicon tracker, which will allow the reconstruction of the particle's impact point on the scintillator bar obtaining the TOF time resolution $\sigma_{tof} = \sqrt{\sigma_t^2 - \sigma_{point}^2}$.

The SAMPIC module was used as the digitizer, with the waveform sampling rate set to 6.4 Gs/s over a 10 ns time window, resulting in a total of 64 samples per signal. The acquisition software was configured to record data only when both channels, corresponding to the signals from the two scintillator bars, exceeded a threshold of 100 mV. Each signal, with amplitudes of several hundred millivolts, was analyzed offline. A constant fraction discriminator (CFD) algorithm was applied to estimate the time difference between the signal arrivals. For a subset of the data, a linear fit to the leading edge of the signal was used to extract the timestamp (figure 3 on the center). Figure 3 (left) shows the distribution of the time difference between the signals from the two scintillators for the two different algorithms. A Gaussian distribution is observed, centered at approximately -1.3 ns, which is attributed to differences in cable lengths used for the two bars. The system measured time resolution is approximately $\sigma_t \sim 144$ ps for the CFD method which corresponds to a resolution on the single bar of $\sigma_t/\sqrt{2} \sim 101$ ps. In the case of linear fit, an improvement in resolution of approximately $\sigma_t/\sqrt{2} \sim 88$ ps (figure 3, right) is obtained.

This preliminary study demonstrates good timing performance. Once the full detector assembly is completed, a new measurement of the time resolution will be performed.

Assuming that the apparatus has a time resolution of a value averaged between the two found above of approximately 90 ps, using the relation:

$$\Delta_t = \frac{L}{pc^2}\left(\sqrt{p^2c^2 + m_p^2c^4} - \sqrt{p^2c^2 + m_\mu^2c^4}\right) \tag{1}$$

putting the distance L between the two scintillators that constitute the TOF at about 30 cm as in the final project, we obtain that we are able to resolve within 3σ a muon ($m_\mu \sim 105.2\,\mathrm{MeV}/c^2$) from a proton ($m_p \sim 938\,\mathrm{MeV}/c^2$) up to pulses of about 1.2 GeV/c.

For higher pulse values, the electromagnetic calorimeter is used to perform PID.

5. Conclusions

The ACROMASS experiment aims to assemble a compact and portable detector capable of performing cosmic ray measurements at ground level across different geographic locations. These measurements are essential for the calibration of atmospheric cosmic ray propagation models used in simulation frameworks. The measurement of the muonic component at ground level is of particular interest for atmospheric neutrino oscillation experiments and for muography applications. Therefore, the ability to discriminate muons from the electronic and protonic components, especially dominant at low energies, is of fundamental importance.

The detector is currently under assembly, and its sub-detectors, the magnetic spectrometer, the TOF system, and the calorimeter, are undergoing testing. In this work, we have presented the TOF sub-detector, which is based on fast plastic scintillators and designed to achieve high time resolution. The goal of this sub-detector is to enable the identification of muons against protons for momenta below 1 GeV/c, down to approximately 100 MeV/c. Signal readout from the SiPMs is handled by the SAMPIC module, a high-performance digitizer capable of time resolutions at the picosecond level.

Based on a preliminary study using a simplified setup compared to the final detector configuration (see section 4), a time resolution of approximately 90 ps was achieved. This timing performance is sufficient to discriminate muons from protons down to momentum of about 1.2 GeV/c with a confidence level of 99.7%.

References

[1] M. Honda *et al.*, *Reduction of the uncertainty in the atmospheric neutrino flux prediction below 1 gev using accurately measured atmospheric muon flux*, *Phys. Rev. D* **100** (2019) 123022.

[2] C. Frosin *et al.*, *Optimizing sea level muon flux modelling: A 2d fit approach and integration into geant4 generators*, *Journal of Physics G: Nuclear and Particle Physics* **32** (2025) 035002.

[3] L. Bonechi *et al.*, *Atmospheric muons as an imaging tool*, *Reviews in Physics* **5** (2020) 100038.

[4] H.K.M. Tanaka *et al*, *Muography*, *Nature Reviews Methods Primers* **3** (2023) .

[5] D. Borselli *et al.*, *Muography as a support technique for non-invasive research and three-dimensional localization of tombs in archaeological sites: a case study from Palazzone Necropolis (Perugia – Italy)*, *Journal of Instrumentation* **19** (2024) C02076.

[6] D. Borselli *et al.*, *Three-dimensional muon imaging of cavities inside the Temperino mine (Italy)*, *Scientific Reports* **12** (2022) 22329.

[7] V. Tioukov *et al.*, *Hidden chamber discovery in the underground hellenistic necropolis of neapolis by muography*, *Scientific Reports* **13** (2023) 5438.

[8] T. Beni *et al.*, *Transmission-Based Muography for Ore Bodies Prospecting: A Case Study from a Skarn Complex in Italy*, *Natural Resources Research* **32** (2023) 1529.

[9] C. Frosin *et al.*, *Exploring the potential of muon radiography for blast furnace assessments: advancements in non-invasive imaging and structural analysis*, *Journal of Instrumentation* **19** (2024) C02041.

[10] S. Navas *et al.,* (Particle Data Group), *Review of Particle Physics*, *Phys. Rev. D* **110** (2024) 030001.

[11] P.K. Grieder, *Cosmic rays at Earth*, Elsevier, Amsterdam (2001).

[12] L. Bonechi *et al.*, *Development of the adamo detector: test with cosmic rays at different zenith angles*, *29th International Cosmic Ray Conference* **9** (2005) 283.

[13] O. Adriani *et al.*, *Pamela measurements of cosmic-ray proton and helium spectra*, *Science* **332.6025** (2011) 69–72.

[14] D. Pagano *et al.*, *EcoMug: An efficient cosmic muon generator for cosmic-ray muon applications*, *Nuclear Instruments and Methods in Physics Research Section A: Accelerators, Spectrometers, Detectors and Associated Equipment* **1014** (2021) 165732.

[15] "EJ-232-Q(0.5) Scintillator, ELJEN Tecnhology." https://eljentechnology.com/products/plastic-scintillators/ej-232-ej-232q, Accessed: July 2025.

[16] "Silicon Photomultipliers Onsemi J-series." https://www.onsemi.com/download/data-sheet/pdf/microj-series-d.pdf, Accessed: July 2025.

[17] D. Breton *et al.*, *Measurements of timing resolution of ultra-fast silicon detectors with the sampic waveform digitizer*, *Nuclear Instruments and Methods in Physics Research Section A: Accelerators, Spectrometers, Detectors and Associated Equipment* (2016) 51–60.

[18] G. Balloni, *Sviluppo del sistema di misura dei tempi di volo per l'esperimento ACROMASS*, *Master Thesis, University of Florence Department of Physics and Astronomy* (2024) .